Trajectory optimization for the planning of percutaneous radiofrequency ablation on hepatic tumors

Claire Baegert*,**, Caroline Villard*, Pascal Schreck*, Luc Soler**, Afshin Gangi***

* LSIIT (UMR 7005 CNRS), Université Louis Pasteur Strasbourg I
Pôle API Boulevard S. Brant, F-67400 Illkirch, France
{baegert,villard,schreck}@lsiit.u-strasbg.fr
**IRCAD, 1 place de l'Hôpital F-67000 Strasbourg, France
***Hôpital Civil, Service de Radiologie B
1 place de l'Hôpital, F-67000 Strasbourg, France

Abstract

Radiofrequency ablation is increasingly used for the treatment of hepatic tumors. Planning the percutaneous intervention is essential and particularly difficult. In this article, we focus on an automated computation of an optimal needle insertion in computer-assisted surgery with 3D visualization. Firstly we recall our method which delimits on the skin of a virtual patient the candidates zones for a needle insertion, *i.e.* those which allow a safe access to the tumor, and then in each one we look for the trajectory minimizing the volume of burnt tissues. Secondly we introduce a quasi-exhaustive method allying sampling and certified minimization to bring a strong argument to the accuracy of our results. We also compare results of both methods on 7 representative reconstructed patient cases.

Keywords: radiofrequency ablation, surgery planning, optimization

1. Introduction

The treatment of hepatic cancers is nowadays mainly surgical. However, many contra-indications remain to liver resection (localization and size of tumor, inoperable patient, etc.). New minimally invasive techniques have been developed in the past few years, in order to be able to treat patients for whom it was not possible to perform open surgery. Among them, we can cite chemo-embolization, cryotherapy, ethanol injection, and radiofrequency ablation (RFA) that appeared to be one of the most secure and easily predictable methods, and that has been increasingly used.

This approach consists in a destruction of the tumor by hyperthermia, using a high-frequency alternative current sent within an electrode inserted in the tumoral tissues. The planning of such an operation takes an important place in its success. Indeed, for a percutaneous RFA, the physician has to choose an accurate strategy for the insertion of the probe, allowing him to destroy the whole tumor while preserving the vital organs of the patient. This step is a delicate issue that is generally performed with only 2D CT scan slices of the patient, or with 2D US views.

We developed a specific planning tool called RF-Sim, aiming at guiding the choice of the physician, giving as many information as possible, and that way reducing the risks of complications and of tumor's recurrence. This program is based on a 3D reconstruction of the organs of the patient, offering an intuitive visualization of his anatomy. RF-Sim is a complete

planning tool that integrates both the visualization of the lesions induced by the treatment, allowing to experiment various strategies, and an automatic planning algorithm proposing optimal trajectories for the needle. One last point of this tool is the realistic simulation of the surgical gesture thanks to a haptic feedback device and virtual reality [1].

In this paper, we will focus exclusively on treatment planning, i.e. computation of an optimal trajectory avoiding vital structures. In the following sections, we will present a brief state of the art and recall the existing functionalities of RF-Sim. Then, we will detail the quasi-exhaustive method we introduced to strengthen the arguments on the accuracy of our results. At last, we will discuss the results and the future extensions of this program.

2. State of the art

The medical literature about RFA is rich [2][3][4][5]. These studies detail the principles of the approach, the contra-indications [6], the characteristics of the different types of devices [7], and the possible complications of the operation [8]. They put forward the common causes of failure [9], and the factors that are possible to modify in order to improve the effects of the treatment [10]. The influence of the human factor has also been evaluated. R. Poon showed in [11] that the chances of success closely depend on the experience of the surgeon. Moreover, G. Antoch underlines in [12] the importance of a volumic visualization of the patient for an adequate placement of the probe inside the tumor during an operation. The elaboration of a program integrating both 3D visualization and planning assistance should contribute to the training of surgeons and improve the success of the operations.

In computer science, many works around planning and simulation of surgical operations can be found. However, RFA being a quite recent technique, there are only a few studies on the simulation and planning of this specific operation. The works presented in [13] and [14] focus on the simulation of the lesion induced by radiofrequency. Thanks to simulations based on FEM, modeling thermal exchanges during the operation, the lesion shape can be evaluated. But within the framework of our program, the described methods would have to be adapted to our constraint of a real-time visualization of the lesion. A. Littmann presents in [15] a software for hepatic resection planning, including the possibility to simulate manually a RFA operation in the case of a non-resectable tumor. A simultaneous 2D/3D visualization and a realistic simulation of the lesion are possible, but the software does not provide the automatic computation of an optimal trajectory for the needle.

We can also mention works about cryoablation, that is an approach rather close to RF treatment. It consists in a destruction of the tumors by chilling instead of heating. The concerns of both techniques are consequently similar in many points. T. Butz presents in [16] a planning tool for cryoablation that is adaptable for RFA, and that integrates the computation of an optimal needle insertion strategy. However, the proposed method is quite time-consuming and requires the prior definition of an insertion window, whereas we want a very quick and fully automatic proposition after a search over the entire abdomen.

3. Our simulator: RF-Sim

The planning software we are developing relies on a method of 3D reconstruction from 2D CT scan slices that is described in [17]. It provides a 3D scene very easy to visualize and manipulate. Moreover, it is possible to introduce in the scene one or more RF probes, to place

them inside the tumor, and to visualize the corresponding lesions. The simulation of cellular heating, the impedance variation and the thermal exchanges within the tissues would allow to determine the exact shape of the produced lesions, but the methods that have been proposed so far do not allow to perform the estimation quickly enough to display the result in real time. S. Mulier details in [18] the properties of the lesions produced by different types of RF needles. The shape of the lesions is predictable and can be assimilated in most cases to a spheroid, the size of which depends on the time the tissues are exposed to heat. In some cases, the proximity of large vessels cools the surrounding area and deforms the shape of the lesion. Therefore, in our simulator the lesion is approximated by a spheroid, and the "heat-sink effect" caused by the blood flow is represented as a "repulsion" of the vertices of the spheroid [19]. This model takes into account a quick and close approximation of main characteristics of the RF burn, and allows to modify interactively the configuration of the probe while visualizing in real time the resulting lesion.

The program also integrates a functionality that computes an optimal position for the needle insertion after the user chooses an initial position [20]. The main criterion for this optimization is the volume of the resulting lesion. Basically, a needle placement will be considered as increasingly interesting when it damages an amount of healthy tissue as small as possible, while still covering the whole tumor. Therefore the purpose is to determine the minimum of a function that associates to each candidate needle position the volume of burnt healthy tissue. However, needle placements that cross organs cannot be considered as appropriate trajectories. In order to eliminate these trajectories that would damage vital organs, the function to minimize is modified by adding them a penalty volume, whatever the burnt healthy tissue volume would be. Among the classical minimization methods [21], the downhill simplex method appeared to be the most efficient, combining at best fast computation with accuracy.

Nevertheless, the obtained result was not fully satisfying. Actually, the resulting position was always interesting, but it was sometimes restricted to a convex zone containing the initial position from which the process was launched. The process had often to face boundaries composed of parts of bones, vessels, or other organs meshes, and was not able to cross them. This was due partly to the optimization method, and partly to the function to minimize. The simplex method is very sensitive to local minima, and the way we added penalties to avoid organs produced a few ones and confined the search within the artificial boundary. In order to find efficiently the optimal trajectory, it was often necessary to try various initial positions. So we could not consider the process as being really fully automatic, while it was one of our goals. We describe in the next sections the solutions we propose to this problem.

4. Candidate zones for the insertion of a needle

The first step of our approach consists in automatically determining the candidate zones of the skin, i.e. zones in which it is possible to insert a needle and to reach the tumor without meeting neither any vital organ nor bones of the patient. Let us recall the algorithm in the following section (more details can be found in [20]).

4.1. Simplified algorithm

In a first step, let us consider the tumor as a single point in space. We will see later how our method is adapted to take into account the actual volume of the tumor.

If we put a virtual camera at the tumor location, each point of the skin visible by the camera and not hidden by any organ, is a possible insertion point. Actually, if there is no obstacle between a point and the tumor, it means that the tumor can be reached without any damage. Still with an idea of efficiency, we considered the skin in terms of a mesh. A triangle of the skin is considered as visible from the tumor, and therefore candidate, if and only if all the points of this triangle are visible. All the points of a candidate triangle are thus possible insertion points.

The visibility of the triangles of the mesh is determined thanks to six renderings of the 3D scene, each one corresponding to one face of a virtual cube located around the tumor. The vision volumes corresponding to the six views allow to cover the whole scene (see Fig.1). That way, whatever the considered triangle of the skin, it is included in one of the views. Then it is possible to compute if it is partially or totally hidden by any organ.

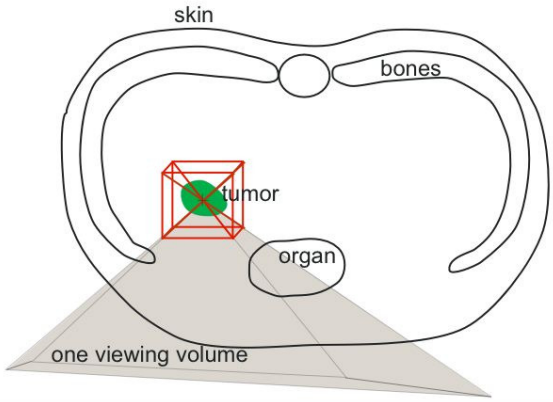

Figure 1 : Covering of the scene with six rendering

This computation is performed very quickly and takes advantage at best of the possibilities of the graphics card. On a Pentium 4 3,2 GHz with a Geforce 7800 GT and 2 Go RAM, the computation time is about 60ms for scenes containing an average of 2000 triangles for the skin and 150000 triangles for the other organs.

4.2. Algorithm taking into account the volume of the tumor

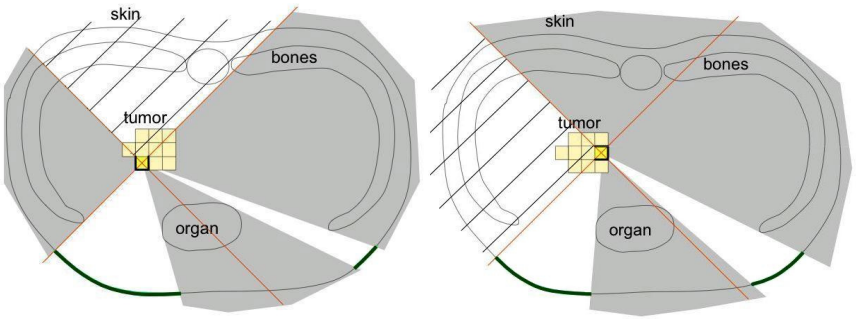

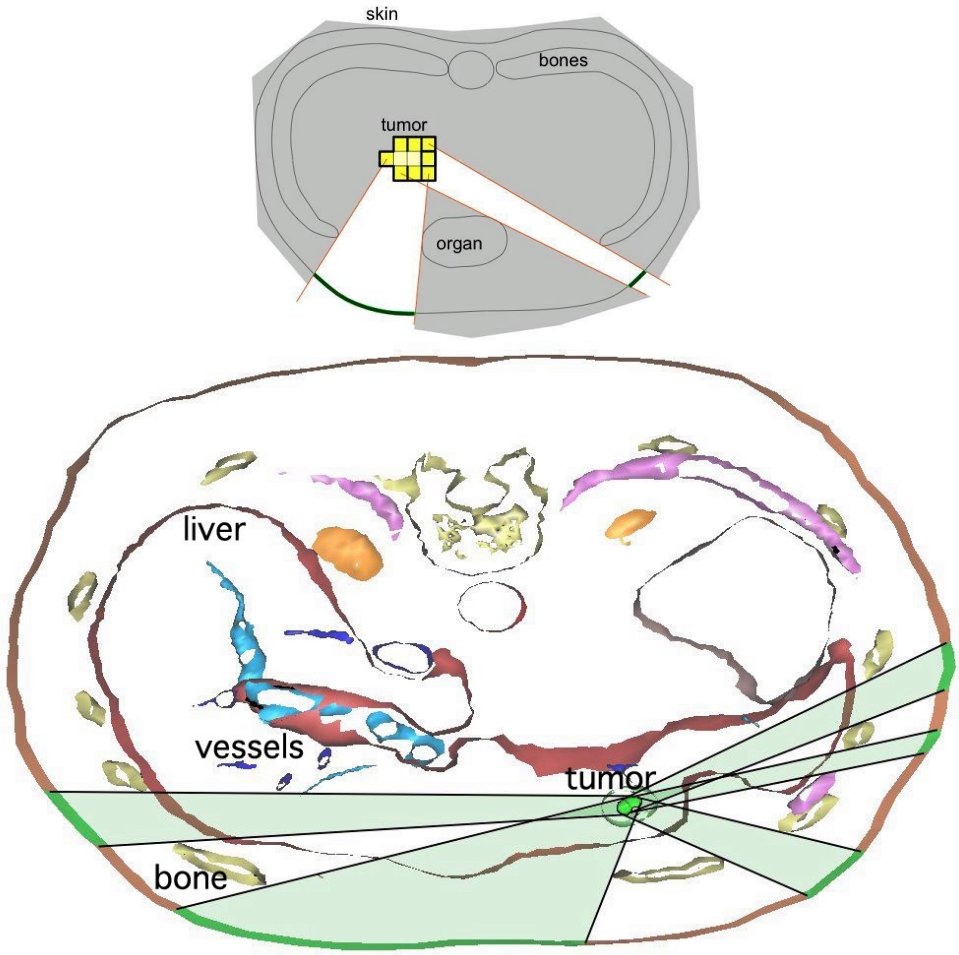

Figure 2: Computation of the 100% zone
2a-b: Visibility zone for 2 different voxels and corresponding views for voxel faces in bold (hatched areas are not considered for these specific voxels).
2c: Resulting 100 % zone once all boundary voxels are studied.
2d: 100% zones on a slice of a virtual patient, reconstructed from a real case.

Now let us detail the modifications on the previous algorithm to take into account the actual volume of the tumor. We could simply use it successively with each voxel constituting the tumor as a point of view. By doing this, we would obtain for each triangle an accessibility rank that would correspond to the ratio of voxels of the tumor that can be seen from the triangle. However, in order to be less time-consuming, we only consider voxels of the tumor's boundary, and among them we only render the views corresponding to faces that are not adjacent to an internal voxel. Indeed, a visibility ray coming from an internal voxel would inevitably pass through an external face, so it is not useful to consider them. We can see on Fig. 2a and Fig. 2b the considered faces for a voxel, and on Fig. 2c all considered faces for this case.

With this optimization, we only obtain an estimation of the accessibility rank. But this does not have any annoying consequences, as we decided for the rest of our works to only consider zones from which it is possible to reach the whole tumor (we will call them the "100% zones"). Indeed, even if it is technically possible to reach some parts of the tumor from some

zones outside the 100% zones (i.e. from partially shaded zones), in practice they would induce trajectories that would be very risky, as they would pass really close to some vital organs. On Fig. 2c, we emphasized the 100% zones, granting a full access to the tumor. In tab.1, the surfaces of the 100% zones corresponding to each case are quite variable, but they are always large enough to enable them to receive the needle insertion safely.

We can notice on Tab.1 that the time taken to compute the 100% zones is strongly correlated with the number of voxels of the tumor's boundary. Actually, this number determines the number of views that have to be computed. The candidate zones on the skin are computed in less than 2 minutes for skin meshes having an average of 2000 triangles, and an average number of voxels of about 600 voxels for the tumors.

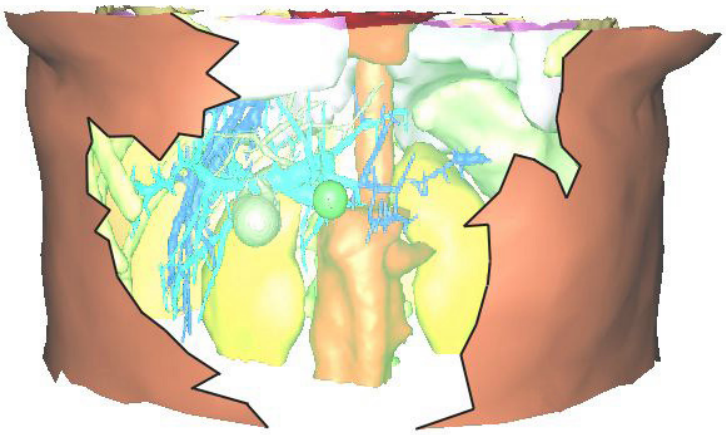

Figure 3: Example of 100% zone

5. Targeted search within the connected components

Once the connected components of the 100% zones are computed, the minimization process has to be launched in each one of them, in order to compare the minima and to choose the optimal trajectory corresponding to the best result. To restrict the search within one of the connected components, we add a penalty to the volume returned by the function to minimize when the trajectory reaches the boundary, as we used to do in our previous method, turning its drawback into an advantage.

In a first approach, we launched one minimization per connected component of the 100% zone with a random initial position for each. As we suspected, the results were satisfying for the convex zones, but in more complex zones we often fell into local minima. To avoid this problem, we added an extra initialization phase to the minimization process. The goal of this initialization phase is to perform a quick evaluation of the best strategy of needle insertion in the component, in order to initialize the position as close as possible to the minimum to find. That way, as the minimization process starts from the appropriate valley, it converges quickly to the accurate minimum, and is prevented to move away to a wrong local minimum.

Here is how the choice of an initial position is performed: the needle tip has to be positioned in the centre of the bounding box of the tumor; then the axis is successively rotated to cross the barycentre of each triangle of the connected component, and the volume of the

corresponding lesion is evaluated; we choose as an initial axis the one providing the smallest volume. The minimization process is then launched from this position. Fig. 4 represents the different trajectories obtained in each of the connected components of the 100% zone.

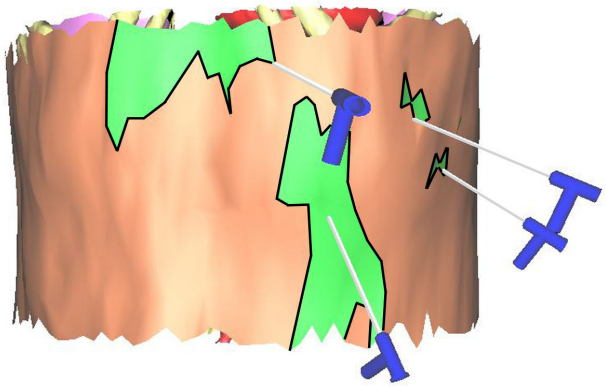

Figure 4: Optimal trajectories in each connected component of the 100% zone

6. Validation of the quality of the results

In order to estimate the reliability and the accuracy of our results and to validate our fast method, we studied a way to compute an accurate approximation of the theoretical minimum of the volume function, in a reasonable time. The computation of the theoretical minimum must avoid undoubtedly all local minima phenomena.

To this end, in a first step, we will show that in our case the problem of local minima of the minimization concerns only the orientation of the needle axis. This provides us a certified minimization if the needle axis is fixed. Then, in a second step, we will explain how we used this property to compute a theoretical minimum with a quasi-exhaustive method allying a sampling of the axis with the certified minimization, and we will use this to evaluate the accuracy of our results.

6.1. No local minima concerning needle tip position

Assuming that the radiofrequency lesion has a spheroid shape and assuming that direction of the needle axis is fixed, the function that associates each needle tip position to the volume of the minimal lesion containing the tumor has only one local minimum, which is of course the absolute minimum. To prove this fact, we use a convexity argument.

The radiofrequency lesion is assimilated to a spheroid centered on the needle tip, its main axis corresponding to the needle axis. The ratio k between short and long radius is fixed. Let us consider a Cartesian coordinate system $(O,x\ y,z)$ such that the x axis corresponds to the fixed needle direction, the equation of the spheroid family that represents the lesion is then:

$$\frac{(x-x_p)^2}{r^2}+\frac{(y-y_p)^2}{k^2.r^2}+\frac{(z-z_p)^2}{r^2}=1$$

where the center of the spheroid $p(x_p, y_p, z_p)$ corresponds to the needle tip. Suppose that point p moves on a line l (not necessarily parallel with the needle axis) that is parametrically defined by:

$$\begin{cases} x(t) = a_0 + b_0.t \\ y(t) = a_1 + b_1.t \\ z(t) = a_2 + b_2.t \end{cases}$$

If we consider the function f_i that associates to each point p on l the radius of the minimal lesion centered in p including a point P_i (x_i, y_i, z_i), we have:

$$f_i^2(t) = (x_i - (a_0 + b_0.t))^2 + \frac{(y_i - (a_1 + b_1.t))^2}{k^2} + (z_i - (a_2 + b_2.t))^2$$

Then, the curve Γ_i that graphically represents function $g_i = f_i^2$, is a concave up parabola (see Fig. 5). We conclude that there is a single value t for which $g_i(t)$ is a minimum, i.e. there is a single position of the needle tip on l that corresponds to a minimal spheroidal lesion including P_i.

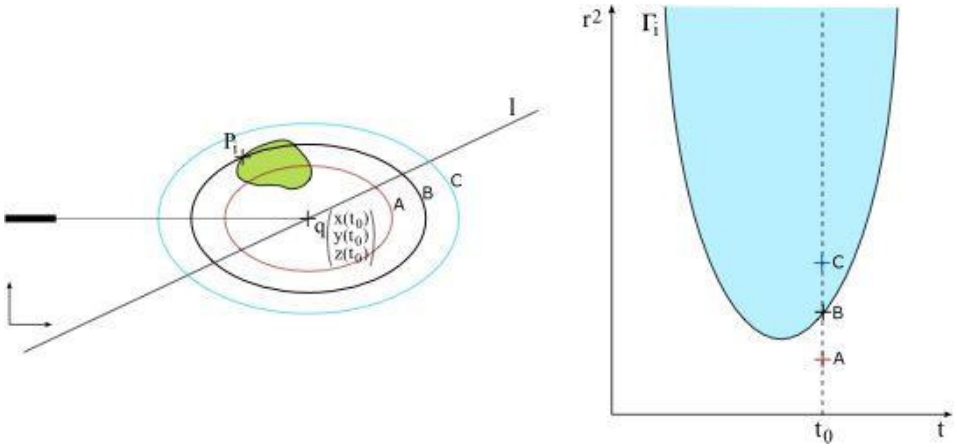

Figure 5: Graphic representation of the function g and its interpretation in space. Spheroids A, B and C in the left part correspond to points A, B and C on the graph.

Spheroids that include all points P_i are also represented by a convex part of the plane because it is the intersection of all convex parts of the plane over parabolas Γ_i. Then we can conclude that for a fixed needle axis there is a unique minimal spheroid placed on l and including all points P_i.

We can extend this by considering now that the needle tip is moving in the entire space (the direction of the needle is already fixed). If we suppose that two different needle tip placements are corresponding to a local minimal volume, then these placements are two points that define a line. That is in contradiction with the above argument. Then we can conclude that for a fixed needle axis, there is a unique needle tip position in the whole space for which the lesion including the entire tumor is a minimum.

6.2. Computation of a theoretical minimum

We have shown that in our case local minima affect only the choice of the needle axis. This information is useful for the computation of a theoretical minimum of our function.

One secure way to find it would be to use an exhaustive method by discretizing the whole parameter space. We tested this method on one patient with a 3° step for the needle axis and considering each tumor voxel as a possible needle tip position. Computation of this minimum took 12 hours and the precision was still low due to the chosen discretization steps.

In fact, a method that would be based upon a discretization of the whole parameter space would have to sample 5 parameters (3 for translation, and 2 for rotation). Such a global sampling leads to a complexity containing a factor in n^5, where n is the chosen number of samples in one dimension. This complexity induces unreasonable computation times. For instance, if we want to double the precision of our sampling, we multiply the computation time by $2^5=32$, giving us a computation time of 384 hours (16 days) instead of 12 hours.

That is why we developed a hybrid method, in order to raise up the precision of our theoretical minimum in a reasonable computation time. Our nearly exhaustive method mixes sampling on the 2 parameters representing the angles with minimization on the 3 parameters representing the position of the needle tip. All angles must be tried for the axis while a minimization method is satisfactory for the needle tip position. By comparing the volumes corresponding to each angle, we can obtain the best one.

Now that we are convinced that when angles are fixed minimization is not subjected to local minima anymore, we can say the error obtained is mainly due to the precision of the sampling on the angles: the precision of the search will mainly depend on the discretization step for the needle axis. With this method, doubling the precision is only 4 times slower.

7. Results

Tab. 2 summarizes the results obtained for 7 test scenes, reconstructed from real patient cases from a Radiology service of Strasbourg's Civil Hospital, having a single tumor located in the liver. It presents the lesion volume resulting of our optimization method (“minimal volume”, 4th column), i.e. the search of a minimum in each connected component we detailed in section 5. We can see the total computation time corresponding to this method in the 3rd column. Let us remark that this computation takes less than 1 minute for all test patients with an average computation time of 4 seconds for each connected component.

These results are compared with our computation of a theoretical minimum. We launched firstly the computation in a scene containing only the tumor, to have an idea of the volume of the minimal spheroid covering the whole tumor if there were no surrounding organ ("global theor. min.", 6th column), then secondly only within the 100% zones ("100% zone theor. min.", 5th column). Execution time was about 2 hours for the global minimum and between 30 minutes and 1 hour for the minimum restricted in 100% zone that is much faster that the exhaustive method while the precision is better.

Firstly we can compare theoretical volumes obtained in 100% zones with global theoretical volumes. We can observe that the search in 100% zones provides volumes having an average increase of +8% with respect to the global theoretical minimum volumes. This phenomenon is mostly inevitable as it is due to the presence of organs obstructing the optimal trajectories. That allows us to mention that the restriction to the 100% zones only adds a small penalty to the obtained volume.

The comparison between results of our minimization and of the computation of a theoretical minimum shows the efficiency of our method, as the results are significantly close (average difference of +0.003mL). In some cases, our method even exceeds the precision obtained by the discretization process we used to compute the theoretical minimum. We conclude that our method provides quickly an estimation of the minimal volume of the lesion and of the corresponding needle placement in the 100% zone with a good precision.

8. Discussion and future works

As we mentioned earlier, in RF-Sim the computation of the optimal position of the needle is mainly based on a volume criterion. However, according to radiologists and surgeons, it is not the only criterion that has to be taken into account for the planning of a RFA operation.

A trajectory considered as optimal by the planning tool could be eliminated by the surgeon, as he may judge it unrealizable, too risky, not easy to reproduce, or simply not practical. Conversely, the physician because of other more interesting properties could choose a trajectory that would lead to a less interesting volume. Various other criteria have to be integrated in the planning tool in order to provide a more realistic assistance, and our tool is only a first step towards this goal.

For instance, we could integrate a degree of risk to needles trajectories that would depend on the distance between the trajectory and the vital organs, allowing a surgeon to choose to give priority to the minimization of risk instead of volume. Or, a surgeon may want to choose the most direct path for the needle, having as a strong concern the minimization of the distance between the insertion point and the tumor. But when the tumor is close to the Glisson's capsule (liver boundary), the needle has to pass through a minimum of healthy part of the liver first, to avoid any hemorrhage. Moreover, the surgeon could choose a totally different solution, having a quite analogous quality, but more compatible with his habits.

Consequently, a maximum of these different criteria involved in the choice of a strategy have to be exhaustively determined in order to be taken into account in the process and to enhance our tool with a larger amount of information, useful to the elaboration of the planning. These information come directly from the expertise of the surgeon. That is why the next step of our works will be to collect from physicists all possible information about the other decisive factors involved in the planning process, and to formalize them so that they will be exploitable in our tool. We also plan to develop methods to materialize intuitively the influence of these factors, either with visual and/or haptic representations.

Moreover, we would like to develop a method that provides a realistic simulation of the lesion by simulating heat production and exchange within the organs. Our current estimation of the RF lesion is advantageous for the computation of the optimal trajectory because of its fastness

but it would be valuable to provide a more precise simulation, at least once a trajectory is chosen.

At last, it would be useful to accelerate the total time necessary to plan an operation. Thanks to the method we presented here, RF-Sim automatically proposes a strategy in less than 5 minutes, but it adds up to the time needed by the 3D reconstruction from 2D CT scan slices. Moreover, in the future we want our tool to handle a lot of other criteria and the planning of several needle insertions, although we would like the whole process to be less than 15 minutes (estimation of a reasonable duration). It will be necessary to keep this constraint in mind in our future developments.

9. Conclusion

We presented in this paper a method computing automatically and quickly an optimal trajectory for the insertion of a needle in the framework of percutaneous RFA. In a first step, our algorithm determines the zones over the skin that can be candidate for an insertion of the needle, then in a second phase it computes an optimal trajectory within each of theses candidate zones, minimizing the volume of the induced lesion, and propose the best one among them. The suggested trajectory is appropriate with respect to the criterion that we imposed: whole tumor burnt, minimum of healthy tissue damaged, vital organs preserved. But this method constitutes a first approach. In our future works we will adapt it in order to take into account various other factors that usually influence the decision of the surgeon during the elaboration of a planning strategy, allowing a more complete approach of each specific operation, and increasing the success rates.

Acknowledgement

We would like to thank Region Alsace for its financial support.

Bibliography

[1] Villard C, Soler L, Gangi A. Radiofrequency ablation of hepatic tumors: simulation, planning, and contribution of virtual reality and haptics. Journal of Computer Methods in Biomechanics and Biomedical Engineering, 2005;8(4):215-227, Taylor and Francis.

[2] McGahan JF, Dodd GD. Radiofrequency ablation of the liver : current status. American Journal of Roentgenology 2001;176:3-16.

[3] Curley A. Radiofrequency ablation of malignant liver tumors. Annals of Surgical Oncology 2003;10:338-347.

[4] Rhim H, Goldberg S-N, Dodd G-D, Solbiati L, Lim HK, Tonolilni M, Cho OK. Essential techniques for successful radio-frequency thermal ablation of malignant hepatic tumors. Radiographics 2001;21:S17-S35.

[5] Ni Y, Mulier S, Miao Y, Michel L, Marchal G. A review of the general aspects of radiofrequency ablation. Abdominal Imaging 2005;30:381-400.

[6] Wood TF, Rose M-D, Chung M, Allegra DP, Foshag L, Bilchik AJ. Radiofrequency of 231 unresectable hepatic tumors : indications, limitations and complications. Annals of Surgical Oncology 2000;7:593-600.

[7] DeBaere T, Denys A, Wood BJ, Lassau N, Kardache M, Vilgrain V, Menu Y, Roche A. Radiofrequency liver ablation : experimental comparative study of water-cooled versus expandable systems. American Journal of Roentgenology 2001;176:187-192.

[8] Mulier S, Mulier P, Ni Y, Miao Y, Dupas B, Marchal G, DeWeber I, Michel L. Complications of radiofrequency coagulation of liver tumours. British Journal of Surgery 2002;89:1206-1222.
[9] Lu D, Raman S, Limamond P, Aziz D, Economou J, Busuttil R, Sayre J. Influence of large peritumoral vessels on outcome of radiofrequency ablation of liver tumors. Journal of Vascular and Interventional Radiology 2003;14:1267-1274.
[10] Goldberg SN. Radiofrequency tumor ablation : principles and techniques. European Journal of Ultrasound 2001;13:129-147.
[11] Poon R, Ng K, Lam C, Ai V, Yuen J, Fan S, Wong J. Learning curve for radiofrequency ablation of liver tumors : prospective analysis of initial 100 patients in a tertiary institution. Annals of Surgery 2004;239:441-449.
[12] Antoch G, Kuehl H, Vogt F, Debation J, Stattaus J. Value of CT volume imaging for optimal placement of radiofrequency ablation probes in liver lesions. Journal of Vascular and Interventional Radiology 2002;13:1155-1161.
[13] Tungjitkusolmun S, Staelin S, Haemmerich S, Tsai JZ, Webster J-G, Lee FT, Mahvi DM, Vorperian VR. Three-dimensional finite element analyses for radio-frequency hepatic tumor ablation. IEEE Transactions on Biomedical Engineering 2002;49:3-9.
[14] Jain MK, Wolf PD. A three-dimensional finite element model of radiofrequency ablation with blood flow and its experimental validation. Annals of Biomedical Engineering 2000;28:1075-1084.
[15] Littmann A, Schenk A, Preim B , Prause GPM, Lehmann K, Roggan A, Peitgen HO. Planning of anatomical resections and in situ ablations in oncologic liver surgery. In : Lemke HU, Vannier MW, Inamura K, Farman AG, Doi K, Reiber JHC, editors : Proceedings of the 17th International Congres of Computer Assisted Radiology and Surgery (CARS 2003), London, June 2003. Elsevier, 2003. p 684-689.
[16] Butz T, Warfield SK, Tuncali K, Silvermann SG, VanSonnenberg E, Jolesz FA, Kikinis R. Pre- and intra-operative planning and simulation of percutaneous tumor ablation. In: Delp SL, DiGioia AM, Jaramaz B, editors: Proceedings of the Third International Conference on Medical Image Computing and Computer-Assisted Intervention (MICCAI 2000), Pittsburgh, October 2000. Springer, 2000. p 317-326.
[17] Soler L, Delingette H, Malandin G. Fully automatic anatomical, pathological and functional segmentation from CT scans for hepatic surgery. Computer Aided Surgery 2001;6:131-142.
[18] Mulier S, Ni Y, Miao Y, Rosière A, Khoury A, Marchal G, Michel L. Size and geometry of hepatic radiofrequency lesions. European Journal of Surgical Oncology 2003;29:867-878.
[19] Villard C, Soler L, Papier N, Agnus V, Gangi A, Mutter D, Marescaux J. RF-Sim: a treatment planning tool for radiofrequency ablation of hepatic tumors. In proceedings of 7th International Conference (IV'2003), Symposium on Information Visualisation in Medical and Biological Sciences (MediVis'03), London, July 2003. IEEE Computer Society Press 2003, p.561-567.
[20] Villard C, Baegert C, Schreck P, Soler L, Gangi A. Optimal trajectories computation within regions of interest for hepatic RFA planning. In :Duncan J, Gerig G, editors: Proceedings of Medical Image Computing and Computer Assisted Intervention (MICCAI'05), Palm Springs, October 2005. LNCS 3750. Springer p. 49-56.
[21] Press W, Teukolsky S, Vetterling W, Flannery B. Minimization or maximization of functions. In Numerical recipes in C++ : the art of scientific computing (2nd edition). Cambridge University Press, 2002, p.394-455.

Table 1 : Results of the computation of the 100% zone			
Case #	Nb of tumor's external voxels	Execution time (s)	Size of 100% zone (cm^2)
1	220	17	234
2	325	21	52
3	401	28	118
4	417	31	165
5	484	32	176
6	1198	82	44
7	1220	81	254

Table 2 : Results of the minimization in each connected component of the 100% zone					
Case #	Nb of connected component of the 100% zone	Our method		Semi-exhaustive method	
		Execution time (s)	minimal volume (mL)	100% Zone min.volume (mL)	Global min.volume (mL)
1	2	6.4	3.07	3.08	2.73
2	5	21.6	2.49	2.48	2.48
3	8	40.6	6.84	6.83	6.83
4	7	23.0	3.83	3.85	3.06
5	5	19.0	3.17	3.16	3.16
6	4	13.0	10.62	10.62	8.86
7	3	11.8	9.32	9.30	9.30